Atmospheric Environment 106 (2015) 382–391

Contents lists available at ScienceDirect

Atmospheric Environment

journal homepage: www.elsevier.com/locate/atmosenv

Volatile organic compound conversion by ozone, hydroxyl radicals, and nitrate radicals in residential indoor air: Magnitudes and impacts of oxidant sources

Michael S. Waring [a, *], J. Raymond Wells [b]

[a] Drexel University, Department of Civil, Architectural and Environmental Engineering, 3141 Chestnut St., Philadelphia, PA 19104, United States
[b] Exposure Assessment Branch, Health Effects Laboratory Division, National Institute for Occupational Safety and Health, 1095 Willowdale Road, Morgantown, WV 26505, United States

HIGHLIGHTS

- Impacts of O_3, OH, and NO_3 on indoor residential VOC conversion were modeled.
- Time averaged equations were used in Monte Carlo modeling for four settings.
- New and established sources of radical oxidants were considered in the modeling.
- Total VOC conversion was dominated by ozonolysis and OH reactions, and not NO_3.
- Source of OH by HONO photolysis was strong, but NO_3 by NO_2 + SCI reactions was not.

ARTICLE INFO

Article history:
Received 28 March 2014
Received in revised form
27 June 2014
Accepted 30 June 2014
Available online 1 July 2014

Keywords:
Indoor chemistry
VOC oxidation
Monte Carlo modeling
Photolysis
Terpenes

ABSTRACT

Indoor chemistry may be initiated by reactions of ozone (O_3), the hydroxyl radical (OH), or the nitrate radical (NO_3) with volatile organic compounds (VOC). The principal indoor source of O_3 is air exchange, while OH and NO_3 formation are considered as primarily from O_3 reactions with alkenes and nitrogen dioxide (NO_2), respectively. Herein, we used time-averaged models for residences to predict O_3, OH, and NO_3 concentrations and their impacts on conversion of typical residential VOC profiles, within a Monte Carlo framework that varied inputs probabilistically. We accounted for established oxidant sources, as well as explored the importance of two newly realized indoor sources: (*i*) the photolysis of nitrous acid (HONO) indoors to generate OH and (*ii*) the reaction of stabilized Criegee intermediates (SCI) with NO_2 to generate NO_3. We found total VOC conversion to be dominated by reactions both with O_3, which almost solely reacted with D-limonene, *and* also with OH, which reacted with D-limonene, other terpenes, alcohols, aldehydes, and aromatics. VOC oxidation rates increased with air exchange, outdoor O_3, NO_2 and D-limonene sources, and indoor photolysis rates; and they decreased with O_3 deposition and nitric oxide (NO) sources. Photolysis was a strong OH formation mechanism for high NO, NO_2, and HONO settings, but SCI/NO_2 reactions weakly generated NO_3 except for only a few cases.

1. Introduction

Indoor volatile organic compounds (VOCs) are oxidized by ozone (O_3), the hydroxyl radical (OH), or the nitrate radical (NO_3). Indoor chemistry research has mostly focused on O_3/terpene reactions, both because O_3 is easy to generate, manipulate, and measure compared to OH and NO_3 and because terpenes are emitted indoors by building materials and consumer products and are often present at significant indoor concentrations (Baumann et al., 1999; Logue et al., 2011; Singer et al., 2006; Toftum et al., 2008). Also, since O_3/terpene reaction rate constants are about 10^{-4}–10^{-2} ppb^{-1} h^{-1}, when viewed within the context of typical indoor O_3 concentrations of ~1–50 ppb, reactions with terpenes compete with loss due to air exchange and influence indoor pollutant loadings (Atkinson and Arey, 2003; Weschler, 2000).

While OH/ and NO_3/terpene reaction rate constants are generally four to five orders of magnitude faster, typical indoor OH concentrations (~10^{-7}–10^{-5} ppb) and NO_3 concentrations (~10^{-6}–10^{-3} ppb) suggest terpenes may react meaningfully with NO_3 as well as O_3 but that reactions of terpenes with OH are too slow to influence terpene conversion for most settings (Nazaroff

* Corresponding author.
E-mail address: msw59@drexel.edu (M.S. Waring).

http://dx.doi.org/10.1016/j.atmosenv.2014.06.062
1352-2310/

and Weschler, 2004; Nojgaard, 2010). However, impacts of all three of these oxidants should be considered because OH and NO_3 can react with many VOCs, in contrast with alkene-only O_3 reactions (Atkinson and Arey, 2003). Therefore, the purpose of this work is to challenge the (perhaps implicit) assumption of a limited indoor reaction scheme based mostly on O_3 and NO_3 reactions with terpenes (and alkenes) and explore total VOC conversion by O_3, OH, and NO_3 in typical indoor environments.

Excellent reviews and investigative research on indoor oxidants are available (e.g. Carslaw, 2007; Drakou et al., 2000; Nazaroff and Weschler, 2004; Sarwar et al., 2002; Weschler, 2000, 2011; Weschler and Shields, 1996, 1997). We recount a brief distillation of this literature regarding the influence of O_3, OH, and NO_3 on VOC conversion and indoor chemistry due to gas-phase reactions. After that, we discuss some new, possibly influential advances in our understanding of sources of oxidants indoors, for both OH and NO_3. Finally, we use a modeling analysis within a Monte Carlo framework to estimate the magnitudes and determinants of gas-phase conversion rates of VOCs due to O_3, OH, and NO_3 in typical residences, and explore the impacts of both the established and newer sources of these oxidants.

1.1. Established background on O_3, OH, and NO_3 sources and reactions

The initiator and main driver of indoor chemistry is O_3, which is largely the result of outdoor-to-indoor transport, and indoor O_3 concentrations are often 20–70% of ambient values (Weschler, 2000). Ozone reacts in the gas-phase with alkenes, or it reacts heterogeneously with building materials or surface-sorbed alkenes, such as squalene or monoterpenes (Atkinson and Arey, 2003; Springs et al., 2011; Wang and Morrison, 2006; Wang and Waring, 2014; Waring and Siegel, 2013; Wells et al., 2008; Weschler, 2000; Wisthaler and Weschler, 2010). However, we focus explicitly on gas-phase oxidation of VOCs. Reaction rates of O_3 and indoor-emitted terpenoids have been widely studied, for instance with D-limonene, α- and β-pinene, terpinolene, γ-terpinene, α-terpineol, linalool, and dihydromyrcenol, among others (e.g. Arey et al., 1990; Atkinson, 1990; Atkinson et al., 1990, 1992b; Forester et al., 2006; Grosjean and Grosjean, 1999; Wells, 2005).

The O_3 reacts with the alkene at the carbon double bond following the so-called Criegee mechanism, forming a primary ozonide that cleaves to yield a carbonyl and an excited Criegee intermediate (CI*), also known as a carbonyl oxide (Atkinson and Arey, 2003; Criegee, 1975). That CI* is either quenched to form a stabilized Criegee intermediate (SCI) that may react with water or an oxygenated organic (the 'SCI channel'); or it can rearrange to form an excited hydroperoxide and then decompose to form an alkyl radical (R•) and OH (the 'hydroperoxide channel') (Atkinson and Aschmann, 1993; Atkinson et al., 1992a; Kroll and Seinfeld, 2008). These O_3/alkene reactions are considered the main driver of indoor OH concentrations; due to their short lifetimes, outdoor-to-indoor transport of OH radicals is not a strong indoor source (Carslaw, 2007; Sarwar et al., 2002; Weschler and Shields, 1996).

OH/VOC reactions lead to the formation of alkyl radicals, alkoxy radicals (RO•), peroxy radicals (RO_2•) and other species which transform by decomposition, isomerization, or hydrolysis, leading to the formation of oxygenated compounds, such as alcohols, carbonyls, carboxylic acids, and hydroxycarbonyls (Atkinson and Arey, 2003; Finlayson-Pitts and Pitts, 2000; Forester et al., 2007; Kroll and Seinfeld, 2008; Orlando and Tyndall, 2012; Orlando et al., 2003; Wells, 2005). Oxygenated organics formed by O_3 or OH reactions can be acute or chronic irritants, and they can sorb to surfaces, oxidize further, contribute to aerosol formation, or be removed by air exchange (Aalto-Korte et al., 2005; Anderson et al., 2007, 2012; Bein and Leikauf, 2011; Jakubowski and Czerczak, 2010; Jarvis et al., 2005; Kroll and Seinfeld, 2008; Weschler, 2011). The quantification of OH indoors is challenging, but OH has been predicted or measured at ~10^{-7}–10^{-5} ppb (Carslaw, 2007; Sarwar et al., 2002; Weschler and Shields, 1996, 1997). OH-driven chemistry could play a minor role in terpenoid conversion indoors (Nazaroff and Weschler, 2004), however a recent investigation by Carslaw (2013) suggests that OH and O_3 contribute more or less equally to D-limonene oxidation.

NO_3 is also formed by O_3 reactions, but in this case from O_3 reacting with NO_2 to yield NO_3 and O_2 (Atkinson et al., 1992b; Nazaroff and Cass, 1986; Weschler et al., 1994). After formation, the NO_3 and remaining NO_2 are in equilibrium with dinitrogen pentoxide (N_2O_5), which can also react with water to form nitric acid (HNO_3) indoors (Weschler et al., 1994). NO_3/VOC reactions yield alkyl, alkoxy, and peroxy radicals, and stable carbonyls and oxygenated compounds that may contain organic nitrate groups (Ham, 2013; Harrison and Ham, 2010; Harrison and Wells, 2012; Jones and Ham, 2008). Organic nitrates are 'under investigated', but research on health effects and indoor NO_x cycles have emphasized the need for more research (Carslaw, 2007; Carslaw et al., 2012). Like OH, NO_3 is difficult to measure; however, modeling and inference experiments have estimated concentrations with an upper bound of ~10^{-3} ppb (Nojgaard, 2010; Weschler et al., 2006). An average NO_3/terpenoid reaction rate constant of ~10^3 ppb^{-1} h^{-1} suggests that NO_3/terpenoid chemistry could impact indoor air (Flemmer and Ham, 2012; Ham, 2013; Harrison and Ham, 2010; Jones and Ham, 2008; Nazaroff and Weschler, 2004).

1.2. Recent advances on OH and NO_3 sources

Recent measurements by Alvarez et al. (2013) have identified photolysis of HONO, which is formed from combustion or NO_2 hydrolysis on indoor surfaces (Finlayson-Pitts et al., 2003; Girman et al., 1982; Spicer et al., 1993; Traynor et al., 1982), as a source of indoor OH. Previously, it was assumed that actinic light fluxes indoors attenuating through windows were not strong enough to photolyze HONO. However, to test for this source, OH, O_3, NO_2, NO and HONO concentrations, relative humidity, and the actinic light flux were monitored over time in a classroom setting (Alvarez et al., 2013). HONO photolyzes at wavelengths of ≤405 nm, and light in the range of 340–405 nm was measured. The authors demonstrated that larger calculated HONO photolysis rates corresponded to observed increases in OH. The Alvarez et al. (2013) experiments suggest the possibility of enhanced OH/VOC chemistry in settings with high concentrations of HONO and/or NO_2 and large indoor actinic fluxes, as also recently discussed by Gligorovski and Weschler (2013).

As discussed above, O_3/alkene reactions form stabilized Criegee intermediates (SCI). While the SCI has been an accepted species for nearly 40 years (Criegee, 1975), its indoor reactive chemistry is now being purposefully investigated. Lifetimes of tens of minutes are estimated for SCIs formed from ozonolysis of alkenes, which implies the possibility of CI*-driven chemistry being influential indoors beyond the 'hydroperoxide channel' OH formation pathway (Mauldin et al., 2012). The SCI has been shown to oxidize sulfur dioxide (SO_2) to sulfuric acid (H_2SO_4), an important species for outdoor particulate matter formation, and also to oxidize NO_2 to NO_3, which would represent a new source of this radical indoors (Mauldin et al., 2012; Ouyang et al., 2013; Taatjes et al., 2013; Welz et al., 2012). Consideration of these new sources of OH and NO_3 implies that NO_2 may play an even more important and central role in the oxidation of VOCs indoors than previously recognized.

2. Modeling methodology

This section uses the reaction information outlined previously to develop modeling to explore the magnitudes and source strengths of O_3, OH, and NO_3 in residential spaces, as well as the magnitudes and determinants of typical VOC conversion rates by those oxidants. Regarding the new sources discussed above, we include OH due to photolysis of HONO generated by deposition of NO_2 to indoor surfaces or from emissions of gas-fired appliances, as well as NO_3 formation due to SCI reactions. Since the focus of this paper is on gas-phase VOC conversion, we ignore the SCI reactions with indoor SO_2 to yield H_2SO_4, as well as products of surface reactions (with the exception of NO_2 deposition to yield HONO).

2.1. Time-averaged model

A time-averaged model was developed to predict the concentrations of O_3, OH, NO_3, NO, NO_2, HONO, N_2O_5, and SCI, based on the 20 reactions in Table 1. Time-averaged equations compute long-term average values and accommodate periodically cycling inputs that are considered as average values (El Orch et al., 2014; Nazaroff and Klepeis, 2003; Riley et al., 2002). Our model is admittedly a simplified representation of the true kinetics and is not explicit. Explicit or semi-explicit models are less appropriate for this type of many-case screening work due to their computational intensity and are better suited for deep investigation (e.g. Carslaw, 2007, 2013; Carslaw et al., 2012; Sarwar et al., 2002, 2003). Other researchers have used models of complexity similar to ours with good success. Weschler and Shields (1996) predicted a typical OH value at 6.7×10^{-6} ppb with a non-explicit model, while Sarwar et al. (2002) with their semi-explicit model predicted OH to be within 0.5% of the Weschler and Shields (1996) concentration for the same model inputs.

To predict O_3, OH, NO_3, NO, NO_2, HONO, N_2O_5, and SCI concentrations, eight time-averaged, mass balances for residences were written, which assume the indoor air is a single well-mixed control volume with air exchange due to a combination of infiltration and natural ventilation. Recirculation air exchange was not considered since we neglect losses within the mechanical system. Some studies have suggested that O_3 can be removed with efficiencies of <~10% by filters in mechanical air handling systems, but these were either conducted with airflow at very low face velocities in laboratory settings or exhibited low O_3 removal (mean removal of <2%) in field settings with single-stage filters (Hyttinen et al., 2003; Zhao et al., 2007). Sorption of VOCs to indoor surfaces is dynamic and not included.

For brevity, we only illustrate a general form of the mass balances used in this work. Time-averaged equations are similar to steady state equations (El Orch et al., 2014; Nazaroff and Klepeis, 2003; Riley et al., 2002), and they are the ratio of the pollutant sources and losses, as demonstrated for a generic pollutant concentration, C_i (ppb), in Equation (1):

$$C_i = \frac{p_i \lambda C_{i,o} + E_i/(V\Gamma_i) + R_{S,i}}{\lambda + \beta_i + R_{L,i}} \quad (1)$$

where λ (h^{-1}) is the air exchange rate; p_i is the penetration factor of i through the building envelope; $C_{i,o}$ (ppb) is the outdoor i concentration; E_i (μg/h) is the emission rate of i; V (m^3) is the building volume; Γ_i is a conversion factor to change units from $\mu g/m^3$ to ppb for i; β_i (h^{-1}) is the deposition rate of i; and $R_{S,i}$ and $R_{L,i}$ are source and loss chemical reactions for i, respectively. The reaction terms depend on the pollutant i but may include gas- or surface-phase reactions, photolysis, or dissociation (see Table 1).

Using the predicted concentrations of O_3, OH, or NO_3, which are C_{O_3}, C_{OH}, and C_{NO_3} (ppb), respectively, the total conversion rate by each oxidant (ox) for all VOCs indoors can be determined by multiplying the respective oxidant concentration, C_{ox} (ppb), by the sum of the products of each VOC concentration j, C_j (ppb), and its reaction rate constant with that VOC, $k_{j\cdot ox}$ (ppb^{-1} h^{-1}). That is:

$$\text{Total VOC conversion rate by each oxidant} = C_{ox} \sum_j (k_{j\cdot ox} C_j) \quad (2)$$

Equation (2) gives an indication of the total effect of an oxidant on indoor gas-phase VOC chemistry, rather than focusing on conversion of a few particular pollutants, such as terpenes alone.

Table 1
Reactions considered in the time-averaged model and their rate constants.

No.	Reaction	Rate constant	Source
1	$O_3 + \text{alkene}_i \rightarrow \text{intermediates} \rightarrow OH + SCI + \text{products}$	Table S1	1
2	$OH + VOC_i \rightarrow \text{products}$	Table S1	1
3	$O_3 + NO \rightarrow NO_2 + O_2$	$k_{NO-O_3} = 1.6$ ppb^{-1} h^{-1}	2
4	$O_3 + NO_2 \rightarrow NO_3 + O_2$	$k_{NO_2-O_3} = 0.0028$ ppb^{-1} h^{-1}	2
5	$OH + NO + M \rightarrow HONO + M$	$k_{NO-OH} = 2800$ ppb^{-1} h^{-1}	2
6	$OH + NO_2 + M \rightarrow HONO_2 + M$	$k_{NO_2-OH} = 5300$ ppb^{-1} h^{-1}	2
7	$OH + NO_3 \rightarrow HO_2 + NO_2$	$k_{NO_3-OH} = 2000$ ppb^{-1} h^{-1}	2
8	$OH + OH \rightarrow H_2O + O$	$k_{OH-OH} = 170$ ppb^{-1} h^{-1}	2
9	$OH + O_3 \rightarrow HO_2 + O_2$	$k_{O_3-OH} = 6.0$ ppb^{-1} h^{-1}	2
10	$NO_3 + VOC_i \rightarrow \text{products}$	Table S1	1
11	$NO_3 + NO \rightarrow 2NO_2$	$k_{NO-NO_3} = 2300$ ppb^{-1} h^{-1}	2
12	$NO_3 + NO_2 \rightarrow N_2O_5$	$k_{NO_2-NO_3} = 180$ ppb^{-1} h^{-1}	2
13	$N_2O_5 \rightarrow NO_3 + NO_2$	$k_{N_2O_5(d)} = 250$ h^{-1}	2
14	$2NO_2(g) + H_2O(aq) \rightarrow HONO(aq) + H^+ + NO_3^-$	Table 2 and $k_{NO_2\cdot surf(HONO)} = 0.055$ h^{-1}	3
15	$NO_2(g) + HONO(aq) \rightarrow H^+ + NO_3^- + NO$	Table 2 and $k_{NO_2\cdot surf(NO)} = 0.055$ h^{-1}	3
16	$HONO(aq) \leftrightarrow HONO(g)$	Not considered in time-averaged model	
17	$HONO + h\nu \rightarrow OH + NO$	Table 2	4
18	$OH + HONO \rightarrow H_2O + NO_2$	$k_{HONO-OH} = 430$ ppb^{-1} h^{-1}	2
19	$SCI + NO_2 \rightarrow NO_3 + \text{products}$	$k_{NO_2-SCI} = 600$ ppb^{-1} h^{-1}	5
20	$SCI + H_2O \rightarrow \text{products}$	$k_{H_2O-SCI} = 0.0089$ ppb^{-1} h^{-1}	5

1. Oxidant/VOC reaction rates are from Atkinson and Arey (2003) and the Master Chemical Mechanism v3.2. See the Supplementary Information for specific information.
2. Atkinson et al., 1992b.
3. Spicer et al., 1993.
4. Alvarez et al., 2013.
5. Welz et al., 2012.

2.2. Monte Carlo method and model input parameters

The model equations were used in four Monte Carlo operations, which run repeated cases of random sampling from probability distributions for input parameters to obtain output distributions, allowing the statistical influence of inputs on results to be quantified. The different Monte Carlo sets considered four residential spaces with different emission scenarios, called R1–R4, including:

- R1: stable indoor background VOCs and variable outdoor O_3 and NO_x concentrations
- R2: stable indoor background VOCs, variable outdoor O_3 and NO_x concentrations, and variable indoor D-limonene concentrations
- R3: stable indoor background VOCs, variable outdoor O_3 and NO_x concentrations, and variable indoor emissions of NO_x and HONO
- R4: stable indoor background VOCs, variable outdoor O_3 and NO_x concentrations, variable indoor D-limonene concentrations, and variable indoor emissions of NO_x and HONO.

We ran 10,000 unique cases for each of the four sets, for which the time-averaged equations were solved simultaneously with an in-house numerical solution program written in the statistical programming software Stata version 11 (StataCorp LP, College Station, TX, USA). Input parameters were best estimates from the literature. Depending on the input parameter type and/or its certainty, some were inputted as single values and some as probability distributions in the Monte Carlo operations.

For reaction rate constants, one value was used based on an indoor temperature of 25 °C (ASHRAE, 2013). Those rate constants are listed in Table 1 for all but the VOC reactions with O_3, OH, and NO_3. Gas-phase reaction rate constants involving oxidation of NO_x and HONO species except for SCI reactions (i.e., Reactions 3–9, 11–13, and 18) were from Atkinson et al. (1992b), while the deposition rate of NO_2 with indoor surfaces (Reactions 14 and 15) and the HONO photolysis rates were inputted as distributions (described below). NO_2 reacts on surfaces with water to produce HONO and NO, and surface production rates were from Spicer et al. (1993). That study reported a value for HONO, but not for NO, so we assumed the same value for NO as HONO production for NO_2 deposition. Gas-phase reactions and rates for SCIs were as in Welz et al. (2012). Due to uncertainty for SCIs from O_3/alkene reactions, we ignored SCI unimolecular decomposition, so the SCI results may be thought of as an upper bound.

Total VOC oxidation rates by O_3, OH, and NO_3 were determined by summing the products of reaction rate constants and median VOC concentrations for typical profiles in residences. The residential VOC concentrations are from Logue et al. (2011), who compiled 91 median concentrations from different studies, and those are listed in the Supplementary Information (SI) in Table S1. Also listed in Table S1 are the oxidant/VOC reaction rate constants, which are from Atkinson and Arey (2003) and the Master Chemical Mechanism v3.2 (Bloss et al., 2005; Jenkin et al., 1997, 2003; Saunders et al., 2003), and molar yields for OH from Weschler and Shields (1996). Additionally, the penetration of O_3 through the building envelope was modeled as constant, starting with the mean value from Stephens et al. (2012) of 0.8 but increasing it to 0.9 because some air exchange in residences is through open windows. The water vapor concentration was set for a relative humidity of 50% at 25 °C.

The Monte Carlo operations used input distributions for the residential air exchange rate and house volume, outdoor O_3 and NO_x concentrations, HONO photolysis rates, deposition rates of O_3 and NO_2 to surfaces, indoor emissions of NO, NO_2, and HONO, and indoor D-limonene concentrations. These parameter distributions were represented as lognormal. Table 2 lists their geometric means (GM) and geometric standard deviations (GSD) and 1st and 99th percentiles.

The air exchange rates, λ (h^{-1}), were fits to values from the Relationship of Indoor, Outdoor and Personal Air (RIOPA) study, which was conducted in the cities of Elizabeth, NJ, Houston, TX, and Los Angeles, CA (Weisel et al., 2005). For R2 and R4 cases, the D-limonene concentration, C_{lim} (ppb), distribution was estimated according to the ranges in the RIOPA study (Weisel et al., 2005), as used in Waring (2014), but truncated so the concentration was never less than the median background D-limonene concentration (2.5 ppb). For R3 and R4 cases, the residential house volume, V (m^3), was estimated from the U.S. American Housing Survey (USBC, 2011) and used with emission rates for a gas-fired burner of NO (89.2 mg/h), NO_2 (136 mg/h) and HONO (3.50 mg/h) from Girman et al. (1982) to determine volume normalized emission rates (E_{NO}/V, E_{NO_2}/V, and E_{HONO}/V), considering the burner was used for two hours per day.

The outdoor O_3 concentration ($C_{O_3,out}$) distribution was the fit of O_3 data from all EPA monitoring stations across the U.S. for 2012 (EPA, 2013). The distributions for the outdoor NO_x concentrations were determined from EPA monitoring data for which there was concurrently available concentrations of NO_2, $C_{NO_2,out}$ (ppb), and NO_x, $C_{NO_x,out}$ (ppb). Using those concentrations, we calculated distributions for $C_{NO_x,out}$ and the ratio of outdoor NO_2 to NO_x, i.e., $C_{NO_2,out}/C_{NO_x,out}$. Then for each modeling case, the $C_{NO_2,out}$ was determined as $C_{NO_x,out} \times (C_{NO_2,out}/C_{NO_x,out})$, and the C_{NO} as $(C_{NO_x,out} - C_{NO_2,out})$.

The distribution for the O_3 deposition rate, β_{O_3} (h^{-1}), was from Lee et al. (1999) and Morrison et al. (2011), and the GM for the NO_2 deposition rate, β_{NO_2} (h^{-1}), was from Spicer et al. (1993) and assumed as having the same GSD as β_{O_3}. Surface deposition rates of radicals OH, NO_3, and SCI were all assumed as having the OH base value of 7.06 h^{-1} from Weschler and Shields (1996) and were varied correspondingly to the O_3 surface deposition rate distribution. The HONO photolysis rate, J_{HONO} (h^{-1}), was estimated from Alvarez et al. (2013), with the GM being the value observed during all times except for in cases of direct light and the 99th percentile being double their maximum observed value (to represent extremely lit rooms). We want to note that this distribution was taken from one study the literature, so there may be some uncertainty in its range; however, we chose this range to explore its potential impact fully.

Table 2
Lognormal parameters (GM = geometric mean; GSD = geometric standard deviation) for input distributions used in the Monte Carlo analysis, as well as their 1st and 99th percentiles.

Parameter	GM	GSD	1st percentile	99th percentile
λ[a] (h^{-1})	0.75	2.1	0.128	4.17
$C_{O_3,out}$[b] (ppb)	25.5	2.31	3.74	142
$C_{NO_x,out}$[b] (ppb)	6.42	3.52	0.349	116
$C_{NO_2,out}/C_{NO_x,out}$[b] (ppb)	0.704	1.41	0.309	0.987
J_{HONO}[c] (h^{-1})	0.2	2.5	0.0239	0.905
β_{O_3}[d,e] (h^{-1})	2.5	1.5	1.08	6.30
β_{NO_2}[f] (h^{-1})	1.18	1.5	0.513	2.94
V[g] (m^3)	387	1.5	153	967
C_{lim}[h] (ppb)	2.5	3.5	2.54	59.0

[a] Weisel et al. (2005).
[b] EPA (2013), monitoring data for 2012.
[c] Alvarez et al. (2013).
[d] Lee et al. (1999).
[e] Morrison et al. (2011).
[f] Spicer et al. (1993).
[g] USBC (2011).
[h] Estimated from Waring (2014), with distribution truncated for concentrations less than 2.5 ppb.

3. Results and discussion

3.1. Oxidant concentrations and source strengths

Fig. 1a shows box plots of the $\log_{10}$ of oxidant concentrations for the four Monte Carlo sets. The boxes show the 25th to 75th percentiles, the median is the line in the box middle, the whiskers are values within 1.5 multiplied by the range of the box, and outliers beyond this range are small circles. For O_3, R1 and R2 cases were similar, and concentrations were between 0.70 and 16 ppb for 10th and 90th percentiles; R3 and R4 were similar and that same range fell to 0.058–11 ppb. These O_3 concentrations are lower than in Lee et al. (2002), who measured a mean of 14.9 ppb, though their outdoor concentrations were much higher at an average of 56.5 ppb. Over all cases, the OH range for the same percentiles was between 4.8×10^{-7} and 8.0×10^{-6} ppb; for NO_3, the range was between 2.3×10^{-8} and 7.1×10^{-5} ppb. The O_3 and OH correspond well to those in previous measurements or modeling (Avol et al., 1998; Sarwar et al., 2002; Weschler, 2000; Weschler and Shields, 1996), but NO_3 is lower than has been suggested by Weschler et al. (2006) and Nojgaard (2010) and is more aligned with concentrations predicted by Carslaw (2007).

The stove emissions in R3 and R4 had a much larger influence on the O_3 concentrations than on the OH or the NO_3 concentrations. The R3 and R4 sets had the lowest average O_3 concentrations because the NO emitted by the gas-fired stove is a dominant O_3 sink. For R1 versus R2, the variable D-limonene concentration had little impact on O_3 overall, since the surface reaction and air exchange losses were more important. The OH concentrations were relatively stable across Monte Carlo sets, but showed a slight trend of R2 > R4, which were both greater than R1 and R3, since there were more O_3/D-limonene reactions in R2 and because OH was formed due to HONO photolysis in R4. The median NO_3 concentration was the greatest for R1, since there was more O_3 available to react with NO_2, though the upper range was higher for R3 for cases with concomitantly high outdoor O_3 and NO_2 emission.

To explore the relative impacts of the different OH and NO_3 formation mechanisms, we show box plots of the distributions of the fractional contribution of each source in Fig. 2. For OH, the sources are (*i*) alkene ozonolysis or (*ii*) HONO photolysis. For R1 and R2, the majority OH source was usually alkene ozonolysis, though HONO photolysis had a sizeable impact and sometimes dominated. The source strengths in R1 and R2 had similar distributions, with differences due to larger R2 D-limonene concentrations. However, for R3 and R4, HONO photolysis was the chief OH source due to the stove use that emitted HONO directly as well as emitted NO_x, which led to NO_2 surface deposition and additional HONO formation indoors. When interpreting this result, please keep in mind that some of our scenarios included values for J_{HONO} from high light fluxes. Regardless, this work shows that this source and its impacts on indoor chemistry deserve serious field investigation in residences with gas appliances.

We also explored the relative source strengths of NO_3 formed by (*i*) O_3/NO_2 reactions, (*ii*) dissociation of N_2O_5 that was formed by NO_3/NO_2 reactions, or (*iii*) SCI/NO_2 reactions. For NO_3 in sets R1–R4, most all formation was due to O_3/NO_2 reactions. The N_2O_5 dissociation was sometimes important in all four sets as well, though it was the strongest in R3 because of high NO_2 due to stove use and subsequent high formation rates of N_2O_5, concurrent with the lowest O_3/VOC reaction rates. Due to the high D-limonene in R2 and R4 sets that led to more SCI formation, the source of NO_3 due to SCI reactions with NO_2 was important for a small number of cases in those sets alone, implying that the SCI source may not be that influential for NO_3 formation in many environments. Shallcross et al. (2014) predicted that high alkene concentrations in the 100 s ppb were necessary for the SCI source to approach the relative

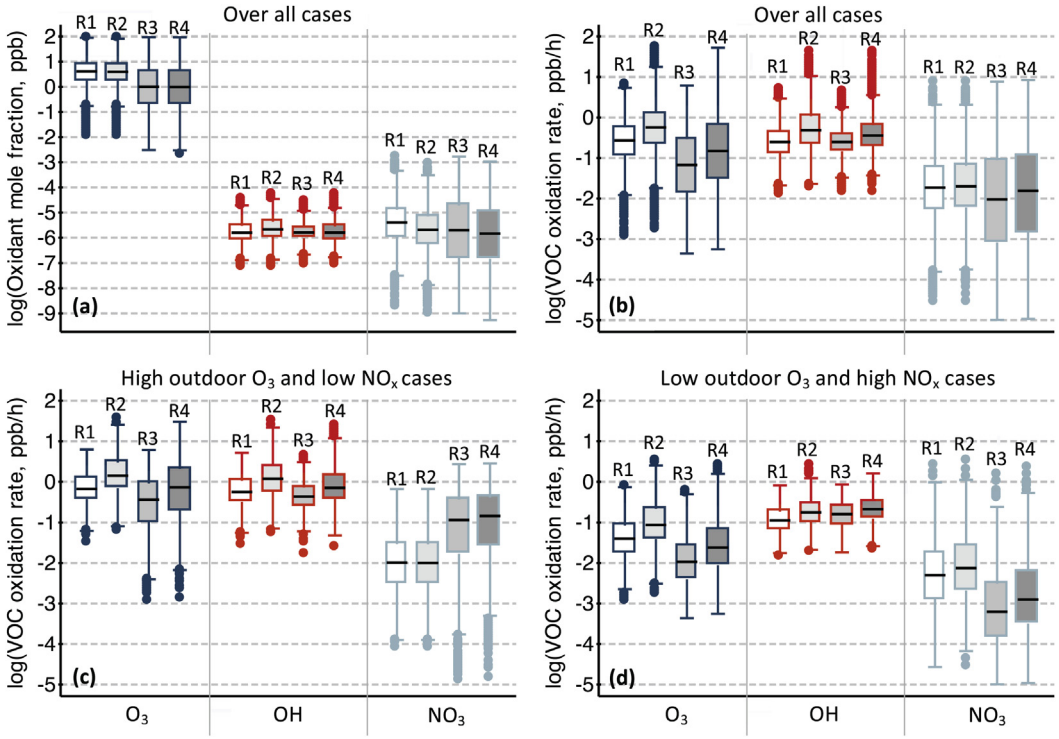

Fig. 1. Box plots of (a) C_{O_3}, C_{OH}, and C_{NO_3} for the different Monte Carlo sets R1–R4; (b) VOC oxidation rate by each oxidant for all cases within each set; (c) VOC oxidation rate by each oxidant for high outdoor O_3 and low outdoor NO_x cases only; (d) VOC oxidation rate by each oxidant for low outdoor O_3 and high outdoor NO_x cases only. See text for more details.

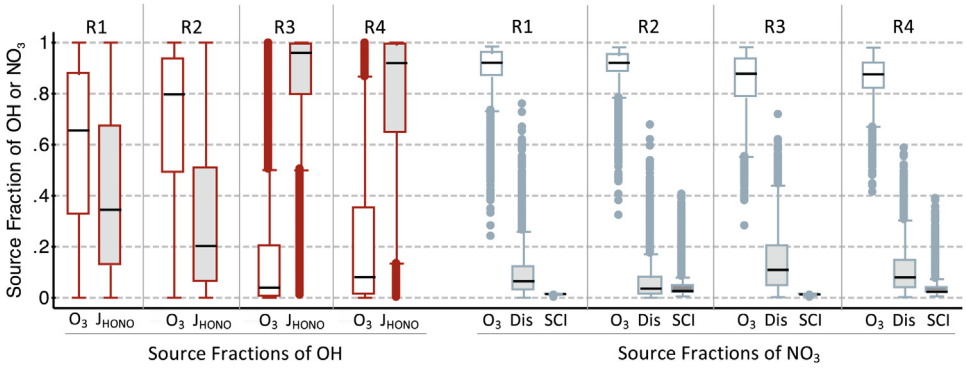

Fig. 2. Box plots of fractions contribution of various OH and NO_3 sources considered in the modeling, for the residential R1–R4 settings. For OH, source 'O_3' is O_3/alkene reactions; 'J_{HONO}' is HONO photolysis. For NO_3, source 'O_3' is O_3/NO_2 reactions; 'Dis' is dissociation of N_2O_5; 'SCI' is SCI/NO_2 reactions.

impact of the O_3/NO_2 source. Correspondingly, in R2 and R4, for SCI source to be responsible for ≥0.3 of the NO_3, the D-limonene concentration was always ≥108 ppb. D-Limonene concentrations such as these or higher can be reached during cleaning events (Singer et al., 2006).

3.2. Total VOC conversion rates

A good metric for an oxidant's influence on indoor chemistry is its total VOC oxidation rate (i.e., as in Equation (2)), and an oxidant's generic impact on concentrations can be first-order approximated by dividing the oxidation rate by the air exchange rate. That is, for an air exchange rate of 0.5 h^{-1}, a total VOC oxidation rate of 0.1 ppb/h would increase generic products by 0.2 ppb. Thus, VOC oxidation rates much lower than this will have little influence on product concentrations. We plotted the $\log_{10}$ of the VOC oxidation rates for sets R1–R4 in Fig. 1b. Results illustrate that OH oxidation is as important as O_3 oxidation, and in R3 and R4 sets with NO_x emissions, the VOC conversion due to O_3 is actually lower than for OH since O_3 reacts strongly with NO. Both have ranges for 25th to 75th percentiles between ~0.01 and 1 ppb/h, and their top 25th percentiles are between ~1 and 100 ppb/h. The VOC oxidation rates by NO_3 are roughly an order of magnitude lower than those for O_3 or OH, suggesting that NO_3 reactions only influence indoor VOC conversion for a small subset of results.

Fig. 1b shows distributions for all 10,000 results for the Monte Carlo sets. However, due to the nature of the outdoor photochemical cycle, it is unlikely that high outdoor O_3 is concomitant with high outdoor NO and NO_2. Typically, in the morning high NO and NO_2 are coincident with low O_3, and in the afternoon this trend is reversed (Seinfeld and Pandis, 2006). To explore these parameter combinations, Fig. 1c and d plot high outdoor O_3/low outdoor NO_x cases and low outdoor O_3/high outdoor NO_x cases, respectively; i.e., cases where the distribution of the ratio of $C_{O_3,out}/C_{NO_x,out}$ was >90th percentile or <10th percentile, respectively. The VOC oxidation by O_3, OH, and even NO_3 was higher in Fig. 1c over d, since indoor oxidative chemistry is driven by O_3. Moreover, when outdoor O_3 is low and NO_x is high, OH/VOC oxidation dominates. For NO_3, the highest rates of VOC conversion are for sets R3 and R4 with the large NO_x stove emissions for the high outdoor O_3/low outdoor NO_x cases.

Fig. 3 shows scatter plots of the VOC oxidation rates as functions of indoor concentrations of O_3, NO, and NO_2 for R2 and R4. These plots are useful to discern how the oxidative capacity of residences is affected by changes in O_3 and NO_x concentrations, which are highly variable. Only 100 cases for each Monte Carlo set are displayed so that trends are discernible. In Fig. 2a and d for both sets, VOC oxidation rates by O_3 and NO_3 are always positively correlated to C_{O_3}; OH is strongly correlated to C_{O_3} for R2 but only weakly for R4, due to the source of OH from photolysis of the HONO in R4. In Fig. 2b and e, all VOC oxidation rates for R2 are uncorrelated to C_{NO}, yet for R4 those by O_3 and NO_3 oxidation are negatively correlated since NO in R4 is high and it is a large O_3 sink. The VOC oxidation by OH is mostly uncorrelated to C_{NO} for R4, which is logical since it was uncorrelated to C_{O_3}. For Fig. 2c and f, the only correlations are between VOC oxidation rates by NO_3 with C_{NO_2} for R2, since there are higher concentrations of O_3 to react with NO_2 to yield NO_3.

3.3. Determinants of oxidant concentrations and total VOC conversion rates

Figs. 1–3 were useful to discern general trends regarding the oxidant concentrations and VOC conversion rates in our results. To explore determinants of the results quantitatively, we conducted a sensitivity analysis. To do so, a multiple linear regression was applied to oxidant concentrations and VOC conversion results for each Monte Carlo set, after natural log-transforming the outcome and predictor variables, which yielded a better fit than regressing non-transformed variables. The predictor variables used in the regressions were {λ, $C_{O_3,out}$, β_{O_3}, $C_{NO,out}$, $C_{NO_2,out}$, β_{NO_2}, J_{HONO}, C_{lim}, E_{NO_Y}/V}, where E_{NO_Y}/V (μg/m^3 h) is the sum of E_{NO}/V, E_{NO_2}/V, and E_{HONO}/V. The resulting coefficients of determination for all 24 regressions were R^2 = 0.72–0.95, with a mean (standard deviation) R^2 = 0.88 (0.070). We only present and discuss R2 and R4.

For our sensitivity analysis, Table 3 lists the standardized regression coefficients (SRC) for R2 and R4 regressions, and their actual regression coefficients are in Table S2 in the SI. The SRC is the actual coefficient normalized by the ratio of the sample standard deviations of the dependent to independent variables. SRCs range from −1 to +1, unless there is a high degree of multicollinearity among the predictor variables (Deegan, 1978), and are useful to compare the relative importance of model inputs on the outcome: a high |SRC| indicates a large influence on the outcome, while a |SRC| near zero indicates no influence, and an input with a −SRC changes the outcome negatively and a +SRC changes the outcome positively. The SRCs for any inputs can be compared, either within one or across different regressions, to quantitatively assess their relative impacts. To aid in the interpretation of SRC results, in Table 3 the SRCs over |0.1| (which are the most influential on the outcome variables) are bolded; also, the greatest positive and negative SRC for each regression is underlined.

We focus on SRCs for the VOC oxidation rates by O_3, OH, and NO_3. The largest +SRCs for VOC oxidation rates by O_3 or OH are

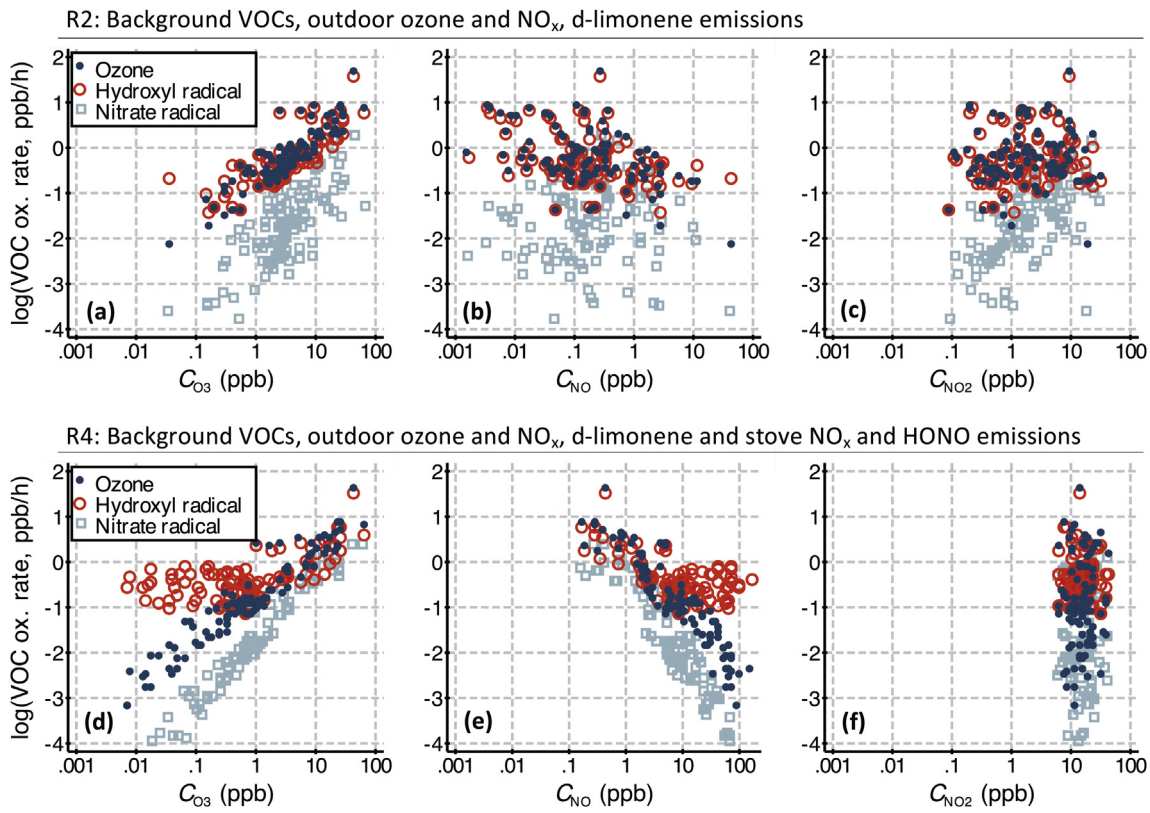

Fig. 3. Scatter plots of the VOC oxidation by O_3, OH, and NO_3 versus C_{O_3}, C_{NO}, and C_{NO_2}, over the R2 and R4 Monte Carlo sets (showing the first 100 cases only for plot clarity).

for inputs of air exchange rate (λ) and outdoor O_3 ($C_{O_3,out}$) and indoor D-limonene (C_{lim}) concentrations, since increases in $\lambda C_{O_3,out}$ directly increase O_3 concentrations and the reactions of O_3/D-limonene increase O_3 oxidation rates while forming OH. However, VOC oxidation by NO_3 is increased by the sources of $\lambda C_{O_3,out}$ and $\lambda C_{NO_2,out}$ but much less by C_{lim}, since increasing D-limonene reduces indoor O_3 and NO_3 formation from ozonolysis of NO_2. The parameter J_{HONO} had a large positive influence for OH/VOC oxidation in R4, due to the photolysis of stove-emitted NO, NO_2, and HONO, though J_{HONO} is less meaningful in R2 without indoor emissions. The largest −SRCs for R2 are for O_3 deposition rates (β_{O_3}), since this parameter reduces the O_3 that is a dominant component of the sources of all oxidants. For R4 for OH/VOC oxidation, the largest −SRC was also β_{O_3}; however, for O_3/and NO_3/VOC oxidation, it was the stove emission (E_{NO_Y}/V) since the emitted NO reduces O_3.

3.4. VOCs most oxidized by O_3, OH, and NO_3 and subsequent products

To contextualize the influences of oxidant/VOC conversion rates on product formation, Table 4 lists for O_3, OH, and NO_3 the ten most oxidized VOCs for the background residential condition, as well as the percentage that each contributes to total VOC oxidation (determined by dividing oxidant-specific VOC reaction rates by the total of that for all VOCs, i.e., $(k_{j\text{-ox}}C_j)/(\sum(k_{j\text{-ox}}C_j))$). For instance, 68%

Table 3
Standardized regression coefficients (SRCs) of natural log-transformed inputs regressed against the natural log-transformed outcome variables for sets R2 and R4. The |SRCs| greater than 0.1 are in bold; the greatest positive and negative SRC for each outcome are underlined. See text for variable and set definitions.

Outcome[a]	Set	λ	$C_{O_3,out}$	β_{O_3}	$C_{NO,out}$	$C_{NO_2,out}$	β_{NO_2}	J_{HONO}	C_{lim}	E_{NO_Y}/V
Standardized regression coefficients for oxidant concentrations for R2 and R4										
C_{O_3}	R2	**0.47**	**0.76**	**−0.21**	**−0.19**	−0.080	−0.00053	−0.0052	−0.037	
	R4	**0.68**	**0.65**	−0.063	−0.088	−0.025	−0.0037	−0.0024	−0.0092	**−0.19**
C_{OH}	R2	**0.45**	**0.78**	**−0.23**	**−0.15**	−0.013	0.034	0.075	**0.17**	
	R4	**0.25**	**0.67**	−0.091	−0.084	−0.0081	**0.12**	**0.42**	−0.00051	−0.059
C_{NO_3}	R2	**0.53**	**0.57**	**−0.15**	−0.065	**0.44**	**−0.12**	−0.0054	**−0.30**	
	R4	**0.66**	**0.65**	−0.061	**−0.10**	0.041	−0.084	−0.0028	−0.095	**−0.15**
Standardized regression coefficients for VOC oxidation rates by oxidant for R2 and R4										
VOC-ox (O_3)	R2	**0.43**	**0.69**	**−0.19**	**−0.17**	−0.073	−0.00090	−0.0045	**0.45**	
	R4	**0.65**	**0.63**	−0.060	−0.085	−0.024	−0.0038	−0.0022	**0.31**	**−0.18**
VOC-ox (OH)	R2	**0.40**	**0.69**	**−0.20**	**−0.13**	−0.012	0.029	0.067	**0.50**	
	R4	**0.23**	**0.61**	−0.082	−0.077	−0.0083	**0.11**	**0.38**	**0.42**	−0.055
VOC-ox (NO_3)	R2	**0.56**	**0.60**	**−0.16**	−0.068	**0.46**	**−0.13**	−0.0055	0.027	
	R4	**0.66**	**0.65**	−0.060	**−0.10**	0.041	−0.085	−0.0027	**0.12**	**−0.15**

[a] Concentrations are units of ppb, oxidation rates in units of ppb/h.

Table 4
Ranking of the ten most important background VOCs for O_3, OH, and NO_3 loss in residences and the percentage of O_3, OH, and NO_3 loss for which those VOCs are responsible.

Rank	O_3/VOC$_i$	% O_3 loss[a]	OH/VOC$_i$	% OH loss[b]	NO_3/VOC$_i$	% NO_3 loss[c]
1	D-Limonene	68%	D-Limonene	24%	D-Limonene	59%
2	α-Pinene	26%	Ethanol	16%	α-Pinene	26%
3	3-Carene	3.3%	Formaldehyde	9.7%	3-Carene	12%
4	Isoprene	1.2%	2-Butanol	9.1%	β-Pinene	1.0%
5	β-Pinene	0.44%	α-Pinene	6.5%	Isoprene	0.96%
6	Styrene	0.38%	Acetaldehyde	6.2%	Styrene	0.48%
7	2-Carene	0.17%	Isoprene	4.1%	Ethanol	0.33%
8	1,3-Butadiene	0.061%	Hexanal	3.4%	2-Carene	0.20%
9	Crotonaldehyde	0.033%	3-Carene	3.4%	2-Butanol	0.074%
10	Acrolein	0.014%	Toluene	1.6%	Acetaldehyde	0.037%

[a] Total loss rate for O_3 to VOCs was 6.6×10^{-2} h^{-1}.
[b] Total loss rate for OH to VOCs was 1.5×10^{5} h^{-1}.
[c] Total loss rate for NO_3 to VOCs was 4.5×10^{3} h^{-1}.

of all O_3 reactions are with D-limonene. Generally, Table 4 demonstrates that D-limonene is the most oxidized VOC by all oxidants; that monoterpenes are largely responsible for O_3 and NO_3 reactions; and that OH reactions are more varied and favor the oxidation of a few monoterpenes, as well as alcohols, aldehydes, aromatics, and isoprene.

Thus, O_3 almost solely reacts with terpenoids, accounting for an average of 99% of O_3 reactions in residences, again with 68% to D-limonene. Since previous analysis demonstrated that O_3/VOC conversion is important for many settings, the products of D-limonene and α-pinene ozonolysis are likely often elevated. These products include very reactive species such as CI*s and SCIs, as well as OH and hydrogen peroxide and other reactive oxygen species (Chen and Hopke, 2010; Li et al., 2002). Stable products include oxygenated organics such as formaldehyde, 4-acetyl-1-methylcyclohexene, limona ketone, and limonaldehyde (Grosjean et al., 1992; Rohr, 2013). Limonene ozonolysis strongly forms secondary organic aerosol (SOA) (Zhang et al., 2006; Waring et al., 2011; Youssefi and Waring, 2014), and Waring (2014) argued that SOA formation in residences could comprise a sizeable fraction of indoor aerosols when O_3 and D-limonene concentrations were high and air exchange rates were low.

Similarly, NO_3 reacts mostly with D-limonene at 59% and also with other monoterpenes. NO_3/terpene oxidation is dominated by NO_3 addition to the unsaturated C=C bond(s), which forms alkyl, alkoxy, and peroxy radicals before ultimately generating nitrated peroxides, carbonyls, and alcohols and SOA (Bolzacchini et al., 2001; Calogirou et al., 1999; Carslaw et al., 2012; Spittler et al., 2006). Jones and Ham (2008) identified those types of nitrated oxygenated products for NO_3/α-terpineol reactions, as well as identified acetone, glyoxal, methyl glyoxal, and others. However, according to the results in Fig. 1b–d, NO_3/VOC oxidation is about an order of magnitude less influential than for O_3 or OH (except for R3 and R4 with indoor NO_x and HONO emissions), so terpene oxidation and product formation will be typically more driven by O_3 or OH than NO_3 in most settings.

OH oxidizes a much richer suite of VOC types than either O_3 or NO_3 in the typical residence herein. OH/D-limonene reactions are still important, though less dominating than for O_3 or NO_3. The OH/terpene reactions generate formaldehyde, acetone, and other carbonyls, as well as larger oxygenated compounds that form SOA (Grosjean et al., 1992; Leungsakul et al., 2005; Wisthaler et al., 2001). Reactions with alcohols are also a dominant OH pathway, leading to carbonyls such as acetaldehyde and propanal or carboxyl acids such as acetic acid (Azad and Andino, 1999). Also, OH/aldehyde reactions yield hydroperoxyl and peroxyl radicals, as well as acylperoxy radicals, which in the presence of NO_2 can form peroxyacyl nitrates (PAN). OH reactions with toluene can yield peroxy and hydroperoxy radicals, as well as dicarbonyls, cresol, alcohols, and SOA (Bloss et al., 2005; Jang and Kamens, 2001; Jenkin et al., 1997, 2003; Saunders et al., 2003).

4. Conclusions

This study investigated the proportional contribution of VOC oxidation indoors by O_3, OH, and NO_3 within typical residences, by using a Monte Carlo-driven modeling effort with time-averaged equations. The model considered established oxidant sources, as well as newly recognized sources of OH and NO_3 indoors, including OH formation due to HONO photolysis and NO_3 formation due to SCI reactions with NO_2. Our model results demonstrated that OH formation due to photolysis could be important relative to alkene ozonolysis, and even be dominant in residences with stove use. The formation of NO_3 by SCI chemistry was not a substantial source for most indoor settings, with some exceptions occurring with high D-limonene concentrations. The VOC oxidation rates by O_3, OH, and NO_3 very generally increased with air exchange, outdoor O_3 and NO_2 concentrations, indoor D-limonene, and HONO photolysis; and they decreased with O_3 deposition and NO sources.

For our inputs, indoor VOC oxidations rates were dominated by O_3 and OH reactions for most settings, though high stove emissions reduced O_3 importance due to scavenging of O_3 by emitted NO. VOC oxidation by NO_3 was about an order of magnitude less influential than O_3 or OH. When outdoor O_3 was high and NO_x was low, VOC oxidation rates by O_3 and OH were very similar, but when outdoor O_3 was low and NO_x was high, OH/VOC oxidation was the stronger of the two. For O_3 and NO_3, reactions with D-limonene dominate the oxidation pathways; for OH, reactions with terpenes, alcohols, aldehydes, and aromatics were all common indoors. The products most likely to increase indoors due to VOC oxidation are from O_3 and OH reactions, and they are various radicals, reactive oxygen species, carbonyls, carboxylic acids, alcohols, and SOA species.

Disclaimer

The findings and conclusions in this report are those of the author(s) and do not necessarily represent the official position of the Centers for Disease Control and Prevention/the Agency for Toxic Substances and Disease Registry. Mention of any commercial product or trade name does not constitute endorsement by the Centers for Disease Control and Prevention/NIOSH.

Acknowledgment

M.S.W.'s contribution to this article is based upon work supported by the National Science Foundation (Grant 1055584).

Appendix A. Supplementary information

Supplementary data related to this article can be found at http://dx.doi.org/10.1016/j.atmosenv.2014.06.062.

References

Aalto-Korte, K., Makela, E.A., Huttunen, M., Suuronen, K., Jolanki, R., 2005. Occupational contact allergy to glyoxal. Contact Dermat. 52, 276–281.

Alvarez, E.G., Amedro, D., Afif, C., Gligorovski, S., Schoemacker, C., Fittschen, C., Doussin, J.-F., Wortham, H., 2013. Unexpectedly high indoor hydroxyl radical concentrations associated with nitrous acid. Proc. Natl. Acad. Sci. U. S. A. 110, 13294–13299.

Anderson, S.E., Franko, J., Jackson, L.G., Wells, J.R., Ham, J.E., Meade, B.J., 2012. Irritancy and allergic responses induced by exposure to the indoor air chemical 4-oxopentanal. Toxicol. Sci. 127, 371–381.

Anderson, S.E., Wells, J.R., Fedorowicz, A., Butterworth, L.F., Meade, B.J., Munson, A.E., 2007. Evaluation of the contact and respiratory sensitization potential of volatile organic compounds generated by simulated indoor air chemistry. Toxicol. Sci. 97, 355–363.

Arey, J., Atkinson, R., Aschmann, S.M., 1990. Product study of the gas-phase reactions of monoterpenes with the OH radical in the presence of NO_x. J. Geophys. Res. Atmos. 95, 18539–18546.

ASHRAE, 2013. In: American Society for Heating, R., and Air-conditioning Engineers (Ed.), Handbook of Fundamentals.

Atkinson, R., 1990. Gas-phase tropospheric chemistry of organic-compounds – a review. Atmos. Environ. A Gen. Top. 24, 1–41.

Atkinson, R., Arey, J., 2003. Gas-phase tropospheric chemistry of biogenic volatile organic compounds: a review. Atmos. Environ. 37, S197–S219.

Atkinson, R., Aschmann, S.M., 1993. OH radical production from the gas-phase reactions of O3 with a series of alkenes under atmospheric conditions. Environ. Sci. Technol. 27, 1357–1363.

Atkinson, R., Aschmann, S.M., Arey, J., Shorees, B., 1992a. Formation of OH radicals in the gas-phase reactions of O_3 with a series of terpenes. J. Geophys. Res. Atmos. 97, 6065–6073.

Atkinson, R., Baulch, D.L., Cox, R.A., Hampson, R.F., Kerr, J.A., Troe, J., 1992b. Evaluated kinetic and photochemical data for atmospheric chemistry supplement-IV – IUPAC subcommittee on gas kinetic data evaluation for atmospheric chemistry. J. Phys. Chem. Ref. Data 21, 1125–1568.

Atkinson, R., Hasegawa, D., Aschmann, S.M., 1990. Rate constants for the Gas-Phase reactions of O-3 with a series of monoterpenes and related-compounds at 296-K +/−2-K. Int. J. Chem. Kinet. 22, 871–887.

Avol, E.L., Navidi, W.C., Colome, S.D., 1998. Modeling ozone levels in and around southern California homes. Environ. Sci. Technol. 32, 463–468.

Azad, K., Andino, J.M., 1999. Products of the gas-phase photooxidation reactions of 1-propanol with OH radicals. Int. J. Chem. Kinet. 31, 810–818.

Baumann, M.G.D., Batterman, S.A., Zhang, G.Z., 1999. Terpene emissions from particleboard and medium-density fiberboard products. For. Prod. J. 49, 49–56.

Bein, K., Leikauf, G.D., 2011. Acrolein – a pulmonary hazard. Mol. Nutr. Food Res. 55, 1342–1360.

Bloss, C., Wagner, V., Jenkin, M.E., Volkamer, R., Bloss, W.J., Lee, J.D., Heard, D.E., Wirtz, K., Martin-Reviejo, M., Rea, G., Wenger, J.C., Pilling, M.J., 2005. Development of a detailed chemical mechanism (MCMv3.1) for the atmospheric oxidation of aromatic hydrocarbons. Atmos. Chem. Phys. 5, 641–664.

Bolzacchini, E., Bruschi, M., Hjorth, J., Meinardi, S., Orlandi, M., Rindone, B., Rosenbohm, E., 2001. Gas-phase reaction of phenol with NO_3. Environ. Sci. Technol. 35, 1791–1797.

Calogirou, A., Larsen, B.R., Kotzias, D., 1999. Gas-phase terpene oxidation products: a review. Atmos. Environ. 33, 1423–1439.

Carslaw, N., 2007. A new detailed chemical model for indoor air pollution. Atmos. Environ. 41, 1164–1179.

Carslaw, N., 2013. A mechanistic study of limonene oxidation products and pathways following cleaning activities. Atmos. Environ. 80, 507–513.

Carslaw, N., Mota, T., Jenkin, M.E., Barley, M.H., McFiggans, G., 2012. A significant role for nitrate and peroxide groups on indoor secondary organic aerosol. Environ. Sci. Technol. 46, 9290–9298.

Chen, X., Hopke, P.K., 2010. A chamber study of secondary organic aerosol formation by limonene ozonolysis. Indoor Air 20, 320–328.

Criegee, R., 1975. Mechanism of ozonolysis. Angew. Chem. Int. Ed. Engl. 14, 745–752.

Deegan, J., 1978. On the occurrence of standardized regression coefficients greater than one. Educ. Psychol. Meas. 38, 873–888.

Drakou, G., Zerefos, C., Ziomas, I., 2000. A sensitivity study of parameters in the Nazaroff-Cass IAQ model with respect to indoor concentrations of O-3, NO, NO_2. Environ. Technol. 21, 483–503.

El Orch, Z., Stephens, B., Waring, M.S., 2014. Predictions and determinants of size-resolved particle infiltration factors in single-family homes in the US. Build. Environ. 74, 106–118.

EPA, 2013. http://www.epa.gov/ttn/airs/airsaqa/detaildata/downloadaqsdata.htm.

Finlayson-Pitts, B.J., Pitts, J.J.N., 2000. Chemistry of the Upper and Lower Atmosphere. Academic Press, New York.

Finlayson-Pitts, B.J., Wingen, L.M., Sumner, A.L., Syomin, D., Ramazan, K.A., 2003. The heterogeneous hydrolysis of NO_2 in laboratory systems and in outdoor and indoor atmospheres: an integrated mechanism. Phys. Chem. Chem. Phys. 5, 223–242.

Flemmer, M.M., Ham, J.E., 2012. Cavity ring-down spectroscopy with an automated control feedback system for investigating nitrate radical surface chemistry reactions. Rev. Sci. Instrum. 83.

Forester, C.D., Ham, J.E., Wells, J.R., 2006. Gas-phase chemistry of dihydromyrcenol with ozone and OH radical: rate constants and products. Int. J. Chem. Kinet. 38, 451–463.

Forester, C.D., Ham, J.E., Wells, J.R., 2007. beta-Ionone reactions with ozone and OH radical: rate constants and gas-phase products. Atmos. Environ. 41, 8758–8771.

Girman, J.R., Apte, M.G., Traynor, G.W., Allen, J.R., Hollowell, C.D., 1982. Pollutant emission rates from indoor combustion appliances and sidestream cigarette smoke. Environ. Int. 8, 213–221.

Gligorovski, S., Weschler, C., 2013. The oxidative capacity of indoor atmospheres. Environ. Sci. Technol. 47, 13905–13906.

Grosjean, D., Williams, E.L., Seinfeld, J.H., 1992. Atmospheric oxidation of selected terpenes and related carbonyls – gas-phase carbonyl products. Environ. Sci. Technol. 26, 1526–1533.

Grosjean, E., Grosjean, D., 1999. The reaction of unsaturated aliphatic oxygenates with ozone. J. Atmos. Chem. 32, 205–232.

Ham, J.E., 2013. Rate constants for the Gas-Phase reactions of ozone and nitrate radicals with the Sesquiterpenes: valencene and farnesol. Int. J. Chem. Kinet. 45, 508–514.

Harrison, J.C., Ham, J.E., 2010. Rate constants for the gas-phase reactions of nitrate radicals with geraniol, citronellol, and dihydromyrcenol. Int. J. Chem. Kinet. 42, 669–675.

Harrison, J.C., Wells, J.R., 2012. 2-Butoxyethanol and benzyl alcohol reactions with the nitrate radical: rate coefficients and gas-phase products. Int. J. Chem. Kinet. 44, 778–788.

Hyttinen, M., Pasanen, P., Salo, J., Bjorkroth, M., Vartiainen, M., Kalliokoski, P., 2003. Reactions of ozone on ventilation filters. Indoor Built Environ. 12, 151–158.

Jakubowski, M., Czerczak, S., 2010. A proposal for calculating occupational exposure limits for volatile organic compounds acting as sensory irritants on the basis of their physicochemical properties. J. Occup. Environ. Hyg. 7, 429–434.

Jang, M.S., Kamens, R.M., 2001. Characterization of secondary aerosol from the photooxidation of toluene in the presence of NO_x and 1-propene. Environ. Sci. Technol. 35, 3626–3639.

Jarvis, J., Seed, M.J., Elton, R.A., Sawyer, L., Agius, R.M., 2005. Relationship between chemical structure and the occupational asthma hazard of low molecular weight organic compounds. Occup. Environ. Med. 62, 243–250.

Jenkin, M.E., Saunders, S.M., Pilling, M.J., 1997. The tropospheric degradation of volatile organic compounds: a protocol for mechanism development. Atmos. Environ. 31, 81–104.

Jenkin, M.E., Saunders, S.M., Wagner, V., Pilling, M.J., 2003. Protocol for the development of the Master Chemical Mechanism, MCM v3 (part B): tropospheric degradation of aromatic volatile organic compounds. Atmos. Chem. Phys. 3, 181–193.

Jones, B.T., Ham, J.E., 2008. alpha-Terpineol reactions with the nitrate radical: rate constant and gas-phase products. Atmos. Environ. 42, 6689–6698.

Kroll, J.H., Seinfeld, J.H., 2008. Chemistry of secondary organic aerosol: formation and evolution of low-volatility organics in the atmosphere. Atmos. Environ. 42, 3593–3624.

Lee, K., Vallarino, J., Dumyahn, T., Ozkaynak, H., Spengler, J., 1999. Ozone decay rates in residences. Air Waste Manag. Assoc. 49, 1238–1244.

Lee, K., Xue, J., Geyh, A.S., Ozkaynak, H., Leaderer, B.P., Weschler, C.J., Spengler, J.D., 2002. Nitrous acid, nitrogen dioxide, and ozone concentrations in residential environments. Environ. Health Perspect. 110, 145–149.

Leungsakul, S., Jaoui, M., Kamens, R.M., 2005. Kinetic mechanism for predicting secondary organic aerosol formation from the reaction of d-limonene with ozone. Environ. Sci. Technol. 39, 9583–9594.

Li, T.H., Turpin, B.J., Shields, H.C., Weschler, C.J., 2002. Indoor hydrogen peroxide derived from ozone/d-limonene reactions. Environ. Sci. Technol. 36, 3295–3302.

Logue, J.M., McKone, T.E., Sherman, M.H., Singer, B.C., 2011. Hazard assessment of chemical air contaminants measured in residences. Indoor Air 21, 92–109.

Mauldin III, R.L., Berndt, T., Sipilae, M., Paasonen, P., Petaja, T., Kim, S., Kurten, T., Stratmann, F., Kerminen, V.M., Kulmala, M., 2012. A new atmospherically relevant oxidant of sulphur dioxide. Nature 488, 193.

Morrison, G., Shaughnessy, R., Shu, S., 2011. Setting maximum emission rates from ozone emitting consumer appliances in the United States and Canada. Atmos. Environ. 45, 2009–2016.

Nazaroff, W.W., Cass, G.R., 1986. Mathematical-modeling of chemically reactive pollutants in indoor air. Environ. Sci. Technol. 20, 924–934.

Nazaroff, W.W., Klepeis, N.E., 2003. Environmental tobacco smoke particles. In: Morawska, L., Salthammer, T. (Eds.), Indoor Environment: Airborne Particles and Settled Dust. Wiley-VCH, Weinheim.

Nazaroff, W.W., Weschler, C.J., 2004. Cleaning products and air fresheners: exposure to primary and secondary air pollutants. Atmos. Environ. 38, 2841–2865.

Nojgaard, J.K., 2010. Indoor measurements of the sum of the nitrate radical, NO_3, and nitrogen pentoxide, N_2O_5 in Denmark. Chemosphere 79, 898–904.

Orlando, J.J., Tyndall, G.S., 2012. Laboratory studies of organic peroxy radical chemistry: an overview with emphasis on recent issues of atmospheric significance. Chem. Soc. Rev. 41, 6294–6317.

Orlando, J.J., Tyndall, G.S., Wallington, T.J., 2003. The atmospheric chemistry of alkoxy radicals. Chem. Rev. 103, 4657–4689.

Ouyang, B., McLeod, M.W., Jones, R.L., Bloss, W.J., 2013. NO_3 radical production from the reaction between the Criegee intermediate CH_2OO and NO_2. Phys. Chem. Chem. Phys. 15, 17070–17075.
Riley, W.J., McKone, T.E., Lai, A.C.K., Nazaroff, W.W., 2002. Indoor particulate matter of outdoor origin: importance of size-dependent removal mechanisms. Environ. Sci. Technol. 36, 200–207.
Rohr, A.C., 2013. The health significance of gas- and particle-phase terpene oxidation products: a review. Environ. Int. 60, 145–162.
Sarwar, G., Corsi, R., Allen, D., Weschler, C., 2003. The significance of secondary organic aerosol formation and growth in buildings: experimental and computational evidence. Atmos. Environ. 37, 1365–1381.
Sarwar, G., Corsi, R., Kimura, Y., Allen, D., Weschler, C.J., 2002. Hydroxyl radicals in indoor environments. Atmos. Environ. 36, 3973–3988.
Saunders, S.M., Jenkin, M.E., Derwent, R.G., Pilling, M.J., 2003. Protocol for the development of the Master Chemical Mechanism, MCM v3 (part A): tropospheric degradation of non-aromatic volatile organic compounds. Atmos. Chem. Phys. 3, 161–180.
Seinfeld, J.H., Pandis, S.N., 2006. Atmospheric Chemistry and Physics. John Wiley & Sons, Inc., Hoboken, N.J.
Shallcross, D.E., Taatjes, C.A., Percival, C.J., 2014. Criegee intermediates in the indoor environment: new insights. Published early online in Indoor Air..
Singer, B.C., Destaillats, H., Hodgson, A.T., Nazaroff, W.W., 2006. Cleaning products and air fresheners: emissions and resulting concentrations of glycol ethers and terpenoids. Indoor Air 16, 179–191.
Spicer, C.W., Kenny, D.V., Ward, G.F., Billick, I.H., 1993. Transformations, lifetimes, and sources of NO_2, HONO, and HNO_3 in indoor environments. J. Air Waste Manag. Assoc. 43, 1479–1485.
Spittler, M., Barnes, I., Bejan, I., Brockmann, K.J., Benter, T., Wirtz, K., 2006. Reactions of NO_3 radicals with limonene and alpha-pinene: product and SOA formation. Atmos. Environ. 40, S116–S127.
Springs, M., Wells, J.R., Morrison, G.C., 2011. Reaction rates of ozone and terpenes adsorbed to model indoor surfaces. Indoor Air 21, 319–327.
Stephens, B., Gall, E.T., Siegel, J.A., 2012. Measuring the penetration of ambient ozone into residential buildings. Environ. Sci. Technol. 46, 929–936.
Taatjes, C.A., Welz, O., Eskola, A.J., Savee, J.D., Scheer, A.M., Shallcross, D.E., Rotavera, B., Lee, E.P.F., Dyke, J.M., Mok, D.K.W., Osborn, D.L., Percival, C.J., 2013. Direct measurements of conformer-dependent reactivity of the Criegee intermediate CH_3CHOO. Science 340, 177–180.
Toftum, J., Feund, S., Salthammer, T., Weschler, C.J., 2008. Secondary organic aerosols from ozone-initiated reactions with emissions from wood-based materials and a "green" paint. Atmos. Environ. 42, 7632–7640.
Traynor, G.W., Girman, J.R., Grimsrud, D.T., Nero, A.V., 1982. Indoor-outdoor air-quality relationships – comments. J. Air Pollut. Control Assoc. 32, 918–919.
USBC, 2011. US Bureau of the Census. American Housing Survey, Washington, DC.
Wang, H., Morrison, G.C., 2006. Ozone-initiated secondary emission rates of aldehydes from indoor surfaces in four homes. Environ. Sci. Technol. 40, 5263–5268.
Wang, C., Waring, M.S., 2014. Secondary organic aerosol formation initiated from reactions between ozone and surface-sorbed squalene. Atmos. Environ. 84, 222–229.
Waring, M.S., 2014. Secondary organic aerosol in residences: predicting its fraction of fine particle mass and determinants of formation strength. Indoor Air. http://dx.doi.org/10.1111/ina.12092 (published early online).
Waring, M.S., Siegel, J.A., 2013. Indoor secondary organic aerosol formation initiated from reactions between ozone and surface-sorbed D-limonene. Environ. Sci. Technol. 47, 6341–6348.
Waring, M.S., Wells, J.R., Siegel, J.A., 2011. Secondary organic aerosol formation from ozone reactions with single terpenoids and terpenoid mixtures. Atmos. Environ. 45, 4235–4242.
Weisel, C.P., Zhang, J.F., Turpin, B.J., Morandi, M.T., Colome, S., Stock, T.H., Spektor, D.M., Korn, L., Winer, A., Alimokhtari, S., Kwon, J., Mohan, K., Harrington, R., Giovanetti, R., Cui, W., Afshar, M., Maberti, S., Shendell, D., 2005. Relationship of Indoor, Outdoor and Personal Air (RIOPA) Study: study design, methods and quality assurance/control results. J. Expo. Anal. Environ. Epidemiol. 15, 123–137.
Wells, J.R., 2005. Gas-phase chemistry of alpha-terpineol with ozone and OH radical: rate constants and products. Environ. Sci. Technol. 39, 6937–6943.
Wells, J.R., Morrison, G.C., Coleman, B.K., 2008. Kinetics and reaction products of ozone and surface-bound squalene. J. ASTM Int. 5, JAI101629.
Welz, O., Savee, J.D., Osborn, D.L., Vasu, S.S., Percival, C.J., Shallcross, D.E., Taatjes, C.A., 2012. Direct kinetic measurements of criegee intermediate (CH_2OO) formed by reaction of CH_2I with O-2. Science 335, 204–207.
Weschler, C.J., 2000. Ozone in indoor environments: concentration and chemistry. Indoor Air Int. J. Indoor Air Qual. Clim. 10, 269–288.
Weschler, C.J., 2011. Chemistry in indoor environments: 20 years of research. Indoor Air 21, 205–218.
Weschler, C.J., Shields, H.C., 1996. Production of the hydroxyl radical in indoor air. Environ. Sci. Technol. 30, 3250–3258.
Weschler, C.J., Shields, H.C., 1997. Measurements of the hydroxyl radical in a manipulated but realistic indoor environment. Environ. Sci. Technol. 31, 3719–3722.
Weschler, C.J., Shields, H.C., Nalk, D.V., 1994. Indoor chemistry involving O-3, NO, and NO_2 as evidenced by 14 months of measurements at a site in southern California. Environ. Sci. Technol. 28, 2120–2132.
Weschler, C.J., Wells, J.R., Poppendieck, D., Hubbard, H., Pearce, T.A., 2006. Workgroup report: indoor chemistry and health. Environ. Health Perspect. 114, 442–446.
Wisthaler, A., Jensen, N.R., Winterhalter, R., Lindinger, W., Hjorth, J., 2001. Measurements of acetone and other gas phase product yields from the OH-initiated oxidation of terpenes by proton-transfer-reaction mass spectrometry (PTR-MS). Atmos. Environ. 35, 6181–6191.
Wisthaler, A., Weschler, C.J., 2010. Reactions of ozone with human skin lipids: sources of carbonyls, dicarbonyls, and hydroxycarbonyls in indoor air. Proc. Natl. Acad. Sci. U. S. A. 107, 6568–6575.
Youssefi, S., Waring, M.S., 2014. Transient secondary organic aerosol formation from limonene ozonolysis in indoor environments: impacts of air exchange rates and initial concentration ratios. Environ. Sci. Technol. http://dx.doi.org/10.1021/es5009906.
Zhang, J., Huff Hartz, K.E., Pandis, S.N., Donahue, N.M., 2006. Secondary organic aerosol formation from limonene ozonolysis: homogeneous and heterogeneous influences as a function of NO_x. J. Phys. Chem. A 110, 11053–11063.
Zhao, P., Siegel, J.A., Corsi, R.L., 2007. Ozone removal by HVAC filters. Atmos. Environ. 41, 3151–3160.